Orbital Domain State and Finite Size Scaling in Ferromagnetic Insulating Manganites

G. Papavassiliou,[1] M. Pissas,[1] M. Belesi,[1] M. Fardis,[1] J. Dolinsek,[2] C. Dimitropoulos,[1,*] and J. P. Ansermet[3,*]

[1]*Institute of Materials Science, NCSR, Demokritos, 153 10 Aghia Paraskevi, Athens, Greece*
[2]*Josef Stefan Institute, Jamova 39, 61111 Ljubljana, Slovenia*
[3]*Department of Physics, University of Illinois, Urbana, Illinois 1801, USA*
(Received 18 October 2002; published 3 October 2003)

^{55}Mn and ^{139}La NMR measurements on a high quality single crystal of ferromagnetic (FM) $La_{0.80}Ca_{0.20}MnO_3$ demonstrate the formation of localized $Mn^{3+,4+}$ states below 70 K, accompanied by a strong cooling-rate dependent increase of certain FM neutron Bragg peaks. $^{55,139}(1/T_1)$ spin-lattice and $^{139}(1/T_2)$ spin-spin relaxation rates are strongly enhanced on approaching this temperature from below, signaling a genuine phase transition at $T_{tr} \simeq 70$ K. The disappearance of the FM metallic signal by applying a weak external magnetic field, the different NMR radio-frequency enhancement of the FM metallic and insulating states, and the observed finite size scaling of T_{tr} with Ca (hole) doping, as observed in powder $La_{1-x}Ca_xMnO_3$ samples, are suggestive of freezing into an inhomogeneous FM insulating and orbitally ordered state embodying "metallic" hole-rich walls.

Understanding the electronic properties of colossal magnetoresistive manganites has been a challenging subject for both experimentalists and theorists, ever since their discovery almost 50 years ago. There are clearly two types of dominant ground states in these compounds: In $La_{1-x}Ca_xMnO_3$ (LCMO), for example, the ground state is ferromagnetic and metallic (FMM) for $0.2 \leq x < 0.5$, and antiferromagnetic insulating for $x \geq 0.5$. The establishment of the FMM phase was initially attributed to the double exchange (DE) interaction [1], i.e., ferromagnetism via the strong Hund's coupling between hopping e_g electrons at neighboring $Mn^{4+,3+}$ sites. However, the detection of FM insulating (FMI) [2] and AFM metallic [3] phases in certain manganites indicates that DE is inadequate for the full description of the magnetic and transport properties in these systems. According to recent theoretical [4–6] and experimental results [2,7], orbital ordering (OO) is an important factor controlling the e_g-hole mobility. A characteristic example is $La_{1-x}Sr_xMnO_3$ (LSMO), where in the doping range $0.1 \leq x \leq 0.15$ a FMM to FMI phase transition takes place at low temperatures [8,9]. Experiments have shown that this transition is associated with charge and orbital ordering, and strong reduction of the cooperative Jahn-Teller (JT) lattice distortions in the low-T phase [2,7,10]. It has been also proposed that the OO phase might contain hole-rich layers [7,11], which sets the question of stripe formation into the FMI phase [6,12].

A similar transition has been observed in LCMO for $0.125 \leq x \leq 0.2$, at $T_{tr} \approx 70–100$ K [13,14]. However, the characteristic resistivity upturn [15–17], which marks the onset of the FMI phase is observed at temperatures sufficiently higher than T_{tr}. Experiments show that the resistivity upturn is associated with a diffuse structural transition, characterized by strong reduction of the orthorhombicity [13], and a remarkable rotation of the easy magnetization axis [17]. These characteristics are considered as the hallmark of orbital rearrangements that take place on cooling. At the same time, a number of peculiar features are observed, which are reminiscent of glassy freezing [18]: (i) a steep decrease and frequency dependence of the ac susceptibility at low temperatures [16,17,19], (ii) strong difference between the field cooled (FC) and zero field cooled (ZFC) magnetization in low fields [17,19–21], (iii) wipeout of the NMR signal, which has been attributed to ultraslow fluctuations of the electronic spin, charge, or orbital degrees of freedom [14,21–24]. On the other hand, the sharp, cooling-rate dependent increase of certain FM Bragg peaks [13] below T_{tr}, indicate rather nonequilibrium phenomena and quasi-nonergodicity ("freezing") on cooling, than a reentrant spin-glass transition. It is the competition between critical slowing down and spin freezing that makes characterization of the spin and orbital dynamics in this system a nontrivial task.

In this Letter we shed light on this intriguing freezing mechanism by using ^{139}La and ^{55}Mn NMR in comparison with recent neutron scattering measurements, performed on the same high quality single crystal of $La_{0.8}Ca_{0.2}MnO_3$. This system exhibits a paramagnetic-to-ferromagnetic transition at $T_c \approx 180$ K, and resistivity upturn at ≈ 150 K. We provide clear evidence about a novel phase transition occurring at $T_{tr} \approx 70$ K. The order of magnitude difference in the rf enhancement of the FMI and FMM NMR signal components, the disappearance of the FMM signal component by applying an external field ~ 0.6 T, and the finite size scaling of T_{tr} upon increasing hole doping, examined on a series of powder LCMO samples in the doping range $0.175 \leq x \leq 0.33$, are indicative of an inhomogeneous OO state with hole-rich walls below 70 K. We anticipate that the spin-freezing features arise from the formation of an intermediate FMI orbital domain state at nanometer length scale. This state is associated with partial magnetic disorder for $T \gtrsim T_{tr}$,

while the establishment of long range OO below T_{tr} is accompanied with better alignment of the Mn electron spins, as deduced from the neutron scattering experiments [13].

Zero external field ^{139}La and ^{55}Mn NMR line shape measurements were acquired by applying a two pulse spin-echo technique, at very low rf power level, due to the very strong rf enhancement that characterizes FM materials [25]. T_1 was measured at the peak of the spectra, by applying a saturation recovery technique and by fitting with a multiexponential recovery law as in previous works [22]. In a similar way, T_2 was measured by applying a two pulse spin-echo technique. Radio-frequency enhancement experiments were performed by recording the NMR signal intensity I as a function of the level of the applied rf field H_1. In general, the obtained curves follow an asymmetric bell-shaped law with maximum at $n\gamma H_1\tau = 2\pi/3$, which allows the calculation of the rf enhancement factor n [25]. The neutron scattering data have been recently reported in Ref. [13].

Figure 1 exhibits ^{55}Mn and ^{139}La NMR line shape measurements at various temperatures. In the case of ^{55}Mn NMR, for $T \geq 70$ K spectra consist of a broad single-peaked line at frequency ≈ 375 MHz, which according to the literature corresponds to delocalized Mn states [14]). For $T \leq 70$ K new peaks increase rapidly on cooling, which correspond to localized Mn^{4+} states (≈ 320 MHz) and Mn^{3+} states (≈ 420 MHz) [14]. Most remarkably, by applying a weak external magnetic field equal to 0.6 T, the FMM signal component disappears, which is typical for signal from FM domain walls. The ^{139}La NMR spectral line shapes do not allow a distinction between FMM and FMI electron states. However, the
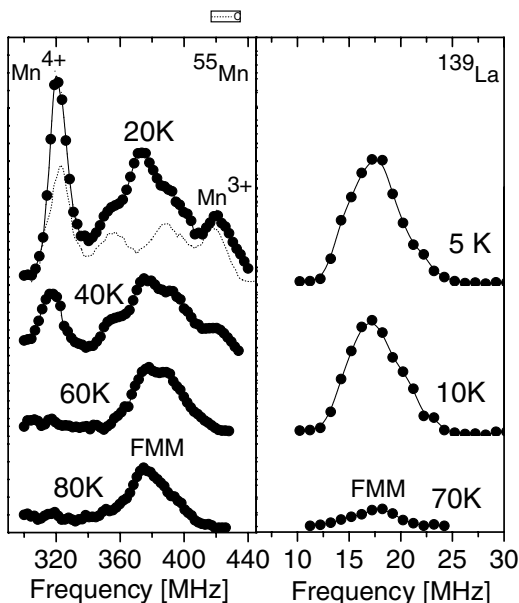
La NMR signal intensity increases rapidly below 70 K, in compliance with the appearance of the ^{55}Mn$^{3+,4+}$ NMR peaks. In the same temperature range, a sharp increase in the intensity of certain ferromagnetic neutron Bragg peaks [Fig. 2(b)] is observed below 70 K on cooling, which implies that the appearance of the localized Mn$^{3+,4+}$ NMR peaks is associated with better ordering of the Mn spins. The intensity of these Bragg peaks depends on the cooling rate as recently reported in Ref. [13]. The rapid increase of the ^{139}La NMR signal from localized electron states below 70 K is also clearly observed in the rf enhancement experiments [Fig. 2(a)]. Specifically, for $T \geq 70$ K only a broad peak with a maximum at 0.3 G is present in the I vs H_1 curves. Below 70 K a second peak at ≈ 2 G appears, which increases rapidly by decreasing temperature. Comparison with Fig. 1 shows that this second peak corresponds to localized Mn$^{3+,4+}$ states, whereas the 0.3 G peak corresponds to delocalized Mn states. The disappearance of the FMM signal component by applying a weak external magnetic field, and the order of magnitude higher rf enhancement of the FMM signal component ($n \approx 3 \times 10^3$), in comparison to the rf enhancement of the FMI one ($n \approx 2 \times 10^2$), indicates that the FMM signal is produced in domain-wall regions,
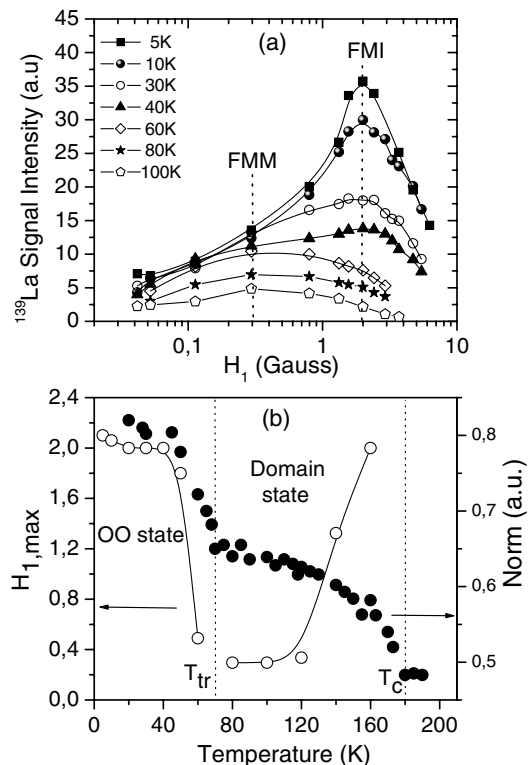

FIG. 2. (a) ^{139}La NMR signal intensity as a function of the rf field H_1 for LCMO $x = 0.20$, at various temperatures. (b) The rf field $H_{1,max}$ of maximum signal intensity as a function of temperature (○), together with the integrated intensity of the (110) [or (002)] Bragg peaks vs temperature (●), from Ref. [13].

FIG. 1. ^{55}Mn and ^{139}La NMR spectra of LCMO $x = 0.20$, at various temperatures. The dotted line at 20 K is the ^{55}Mn line shape in external field 0.6 T, magnified $5 \times$.

while the FMI signal in domains [25]. Finite size scaling arguments given below support this interpretation.

Figure 3 shows $^{55,139}(1/T_{1,2})$ measurements as a function of temperature. In the case of $^{55}(1/T_1)$ measurements were performed on the Mn^{4+} peak and the central FMM peak, whereas in case of $^{139}(1/T_{1,2})$ measurements were performed at rf power levels 0.3 and 2 G, which correspond to delocalized and localized ($Mn^{3+,4+}$) states, respectively. The crucial point in Figs. 3(a) and 3(b) is that $1/T_{1,2}$ from $Mn^{3+,4+}$ ions are strongly enhanced on approaching 70 K from below. Such a behavior characterizes the onset of structural and magnetic rearrangements as $T \rightarrow T_{tr}$. On the other hand, the FMM $1/T_{1,2}$ relaxation rates show only a small hump at ≈ 25 K, while at temperatures higher than 70 K, where the FMI signal is completely wiped out [22,23], the relaxation rates reflect solely the dynamics of the FMM states. The wipeout effect and the $^{139}(1/T_2)$ enhancement as $T \rightarrow T_{tr}$ is also demonstrated in powder LCMO samples for $0.175 \leq x \leq 0.25$ (Fig. 4). However, in this case the relaxation enhancement is observed as a broad maximum, because in nonoriented powder samples the effective rf field H_1, varies in differently oriented grains, and therefore there is signal contribution from both FMI and FMM regions at all rf power levels.

In a recent neutron scattering study (performed on the same $x = 0.20$ crystal as here [26]) two different FM media were detected, which coexist dynamically in the temperature range $T_{tr} \leq T \leq T_c$, and are frozen into a periodically arranged collective state below T_{tr}. Our NMR results in conjunction with this finding provide evidence that at low temperatures the system consists of a regular arrangement of FMI (OO) domains separated by FMM walls. In order to envisage how such an orbital domain state could be realized, we consider the idea of the random field Ising model [27,28], where the random field mimics the lattice distortions induced by substitution with Ca ions. By taking into account only the isospin $S = 1/2$ degree of freedom, which describes the twofold e_g orbital degeneracy [4,5], it can be shown that in strong random fields an intermediate orbital domain state may be realized on cooling [29–31]. This state is metastable exhibiting anomalous slow relaxation with logarithmic time dependence [32,33] and strong difference in the orbital and spin ordering between the ZFC and FC branches [29]. The observed cooling-rate dependence of the FM Bragg peak intensity below T_{tr} is attributed to nucleation or rearrangement of orbital domains and domain walls, which is connected with the large reduction of orthorhombicity upon cooling [13]. We also note that in the case that neighboring orbital domains are arranged in antiphase, stripelike orbital walls would be formed, where holes are energetically favorable to concentrate [12], in agreement with the neutron measurements [26]. By increasing hole doping the number of walls will increase [12], whereas above a critical doping x_c the OO phase is expected to be suppressed [34,35]. Indeed, such doping induced finite size scaling effects are experimentally
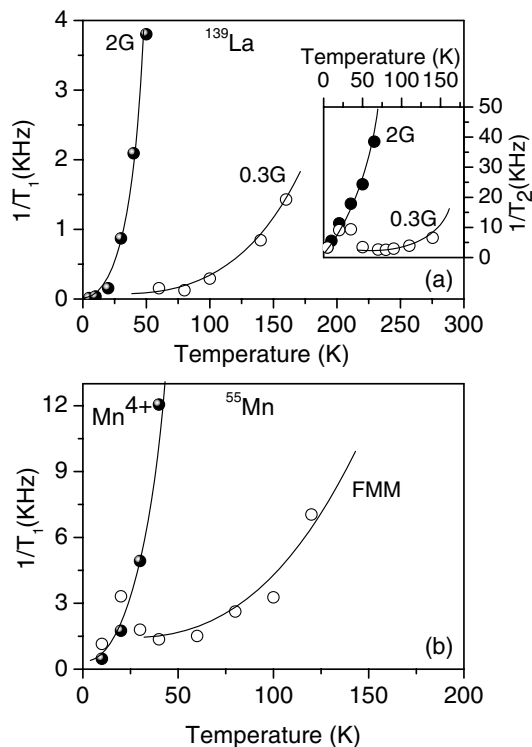

FIG. 3.   (a)$^{139}(1/T_1)$ and $^{139}(1/T_2)$ (inset) of LCMO $x = 0.20$, (b)$^{55}(1/T_1)$ of $La_{0.80}Ca_{0.20}MnO_3$ as a function of temperature.
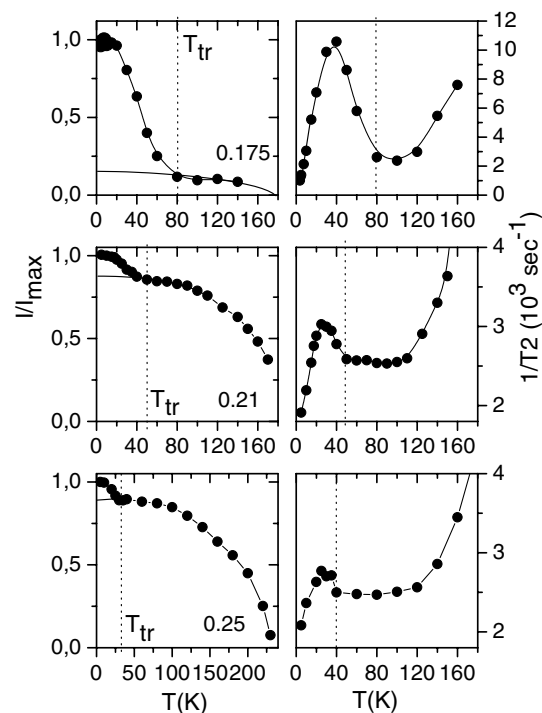

FIG. 4. ^{139}La NMR signal intensity and $^{139}(1/T_2)$ as a function of temperature of powder samples with $x = 0.175$, 0.21, and 0.25.
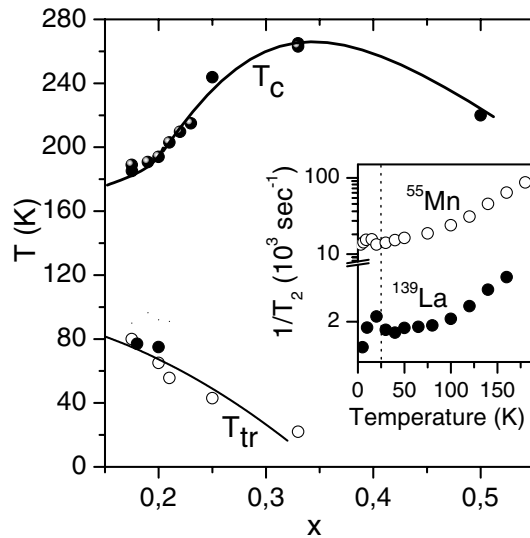
FIG. 5. The magnetic phase diagram of LCMO in the doping range $0.175 \leq x \leq 0.5$. Experimental points were obtained by NMR (○) and magnetic measurements (●). The inset shows $^{55,139}(1/T_2)$ for $x = 0.33$. The lower solid line is theoretical fit on T_{tr} as described in the text.

suggested. Figure 5 shows the magnetic phase diagram and T_{tr} vs doping x. It is worth noting that contrary to current belief, the transition to the low-T OO state is present even for $x = 0.33$, i.e., deep into the FMM phase, as shown by the inset in Fig. 5. The experimental data may be fitted by the expression $T_{tr}(x) = T_{tr}^*[1 - (x/x_c)^n]$, where $T_{tr}^* = 100$ K, $x_c = 0.35$, and $n = 2$. Such a power-law dependence is expected by finite size scaling theory [34,35], which predicts that the effective T_{tr} is limited by the finite size L of the domains according to the formula, $T_{tr}(L) = T_{tr}(\infty)[1 - (L/L_0)^{-1/\nu}]$. The above equations are consistent with $L(x) \approx 1/x^{n\nu}$, which is determined as evidence about the formation of walls separating orbital domains. Considering the mean-field approximation $\nu = 1/2$, it is obtained $L(x) \approx 1/x$, i.e., the wall width would be independent of x, in accordance with recent theoretical predictions [12].

In summary, NMR experiments on single crystalline LCMO $x = 0.20$ correlate excellently with recent neutron scattering experiments on the same crystal, and provide evidence about freezing into an inhomogeneous OO state comprising FMI domains separated by FMM walls. Although no direct evidence about stripe formation is claimed here, the finite size scaling behavior of the transition temperature T_{tr}, as obtained from LCMO samples for $0.175 \leq x \leq 0.33$, suggests that the formation of the domain state and the orbital and spin-freezing effects are possibly associated with the formation of hole stripes. By assigning the e_g orbital degree of freedom to an isospin, there is a complete analogy between the OO phase in manganites and the low temperature hole-striped phase in cuprates and nickelates [35,36]. This is probably due to the similar competitive spin (isospin) ordering under

quenched disorder [37] in layered (2D) structures. Clearly, further investigations of the orbital and spin dynamics in lightly doped manganites will be particularly helpful in understanding the way that holes are self-assembled in these systems.

*Permanent address: Institut de Physique Exprimentale, EPFL-PH-Ecublens, 1015-Lausanne, Switzerland

[1] C. Zener, Phys. Rev. **82**, 403 (1951).
[2] Y. Endoh *et al.*, Phys. Rev. Lett. **82**, 4328 (1999).
[3] R. Kajimoto *et al.*, Phys. Rev. B **60**, 9506 (1999).
[4] Y. Tokura and N. Nagaosa, Science **288**, 462 (2000).
[5] E. Dagotto *et al.*, Phys. Rep. **344**, 1 (2001).
[6] T. Mizokawa *et al.*, Phys. Rev. B **61**, R3776 (2000).
[7] Y. Yamada *et al.*, Phys. Rev. Lett. **77**, 904 (1996).
[8] G.-L. Liu *et al.*, Phys. Rev. B **64**, 144414 (2001).
[9] J.-S. Zhou *et al.*, Phys. Rev. B **62**, 3834 (2000).
[10] Y. Yamada *et al.*, Phys. Rev. B **62**, 11 600 (2000).
[11] T. Inami *et al.*, Jpn. J. Appl. Phys., Suppl. **38-1**, 212 (1999).
[12] T. Hotta *et al.*, Phys. Rev. Lett. **86**, 4922 (2001).
[13] G. Biotteau *et al.*, Phys. Rev. B **64**, 104421 (2001).
[14] G. Papavassiliou *et al.*, Phys. Rev. Lett. **84**, 761 (2000).
[15] T. Okuda *et al.*, Phys. Rev. B **61**, 8009 (2001).
[16] V. Markovich *et al.*, Phys. Rev. B **65**, 144402 (2002).
[17] V. Markovich *et al.*, Phys. Rev. B **66**, 094409 (2002).
[18] P. Dai *et al.*, Phys. Rev. Lett. **85**, 2553 (2000).
[19] R. Laiho *et al.*, Phys. Rev. B **63**, 094405 (2001).
[20] C. S. Hong *et al.*, Phys. Rev. B **63**, 092504 (2001).
[21] M. Belesi *et al.*, Phys. Rev. B **63**, 180406R (2001).
[22] G. Papavassiliou *et al.*, Phys. Rev. Lett. **87**, 177204 (2001).
[23] G. Allodi *et al.*, Phys. Rev. Lett. **87**, 127206 (2001).
[24] M. M. Savosta *et al.*, Phys. Rev. B **67**, 094403 (2002).
[25] G. Papavassiliou *et al.*, Phys. Rev. B **55**, 15000 (1997).
[26] M. Hennion *et al.*, cond-mat/0112159.
[27] S. Fishman and A. Aharony, J. Phys. C **12**, L729 (1979).
[28] R. Bruinsma and G. Aeppli, Phys. Rev. Lett. **52**, 1547 (1984).
[29] C. Ro *et al.*, Phys. Rev. B **31**, R1682 (1985).
[30] Po-zen Wong and J.W. Cable, Phys. Rev. B **28**, R5361 (1983).
[31] H. Yoshizawa and D. P. Belanger, Phys. Rev. B **30**, 5220 (1984).
[32] T. Nattermann and I. Vilfan, Phys. Rev. Lett. **61**, 223 (1988).
[33] J. Villain, Phys. Rev. Lett. **52**, 1543 (1984).
[34] M. E. Fisher and M. N. Barber, Phys. Rev. Lett. **28**, 1516 (1972).
[35] J. H. Cho *et al.*, Phys. Rev. Lett. **70**, 222 (1993).
[36] J. M. Tranquada *et al.*, Nature (London) **375**, 561 (1995); J. M. Tranquada *et al.*, Phys. Rev. Lett. **73**, 1003 (1973).
[37] J. Burgy *et al.*, Phys. Rev. Lett. **87**, 277202 (2001).